Creation of an Atomic Superlattice by Immersing Metallic Adatoms in a Two-Dimensional Electron Sea

Fabien Silly,[1,*] Marina Pivetta,[1] Markus Ternes,[1] François Patthey,[1] Jonathan P. Pelz,[2] and Wolf-Dieter Schneider[1]
[1]*Institut de Physique des Nanostructures, Ecole Polytechnique Fédérale de Lausanne (EPFL), CH-1015 Lausanne, Switzerland*
[2]*Department of Physics, The Ohio State University, Columbus, Ohio 43210, USA*
(Received 27 May 2003; published 9 January 2004)

Cerium adatoms, deposited on a Ag(111) surface, are found by low-temperature scanning tunneling microscopy to self-assemble into large ordered hexagonal arrays covering macroscopically the entire surface. We show that the 32 Å periodicity of the superlattice is caused by the interaction of surface-state electrons with Ce adatoms and that the large-scale formation of the superlattice is governed by a subtle balance between the sample temperature, the surface diffusion barrier, and the concentration-dependent adatom interaction potential.

DOI: 10.1103/PhysRevLett.92.016101 PACS numbers: 68.43.Hn, 68.37.Ef, 73.20.At

The control of the geometric, electronic, and magnetic properties of arrays of atomic-scale nanostructures is a prerequisite for the understanding and fabrication of new materials and devices. Two routes lead towards this goal, the sequential manipulation of single atoms and molecules with the scanning tunneling microscope (STM) [1–4] or patterning using self-assembly [5–7]. One proposed mechanism for atomic self-assembly was long-range (10–30 nm) surface-state-mediated adatom interactions [8] that have been found on metal surfaces [9–12]. In this scenario, the surface-state electrons attempt to screen the impurity represented by an adatom, giving rise to surface-state Friedel oscillations. Because of the Fermi cutoff in momentum space, not all the wave vectors contribute to the screening process [13]. As a result, at the Fermi energy (E_F) the local density of states (LDOS) oscillates around the impurity with a wavelength of $\lambda_F/2 = \pi/k_F$, where λ_F is the Fermi wavelength and k_F the Fermi wave vector. This variation of the LDOS at E_F due to standing-wave formation modifies the adsorption energy of the adsorbates. For adatoms it appears to be energetically favorable to rest in regions of high LDOS at E_F. Therefore the interaction between the adsorbates, and consequently their mutual distance, is determined by the LDOS at E_F. The interaction energy decays as $1/\rho^2$ where ρ is the distance between two adatoms, and oscillates with a period of $\lambda_F/2$, half of the Fermi wavelength of the surface-state electrons [14,15]. In these models, an important parameter is the scattering phase shift δ_0 at the Fermi level E_F, which determines the position of the first maximum in the LDOS and of the first minimum in the adatom-adatom interaction potential.

While the experiments of Refs. [11,12] showed the existence of the long-range interactions mediated by the surface-state electrons, they were not successful in producing a large ordered superlattice. Repp *et al.* [11] observed near a step edge on a Cu(111) surface that the copper adatoms, at low coverage, form a small island with a local hexagonal structure. However, at distances far away from a step edge, such an island was not observed [16]. Knorr *et al.* [12] investigated the adatom-adatom interaction of Cu and Co on Cu(111) and Ag(111) surfaces at higher adatom concentration because they were aware of the possibility of the creation of a superlattice with a lattice constant given by the first minimum of the adatom-adatom interaction energy. However, no superlattice was observed.

Here we report on the realization of a hexagonal two-dimensional superlattice of metallic Ce adatoms, by taking advantage of the long-range adatom-adatom interactions mediated by a two-dimensional electron gas. In our measurements and analysis, we determine directly the superlattice confining potential by making a detailed statistical analysis of the mobile Ce atoms as they hop around the nominal threefold coordinated lattice sites, while the earlier studies [10–12] were able to estimate only the nearest neighbor pairwise interactions. We demonstrate that a subtle balance of temperature, surface diffusion barrier, and concentration-dependent adatom interaction potential is decisive for the formation of the superlattice. Therefore, our realization of a hexagonal superlattice constitutes a novel method for achieving ordered overlayer structures. This adatom superlattice might be exploited in heterogeneous catalysis, thin film epitaxy, and molecular self-assembly [17].

Ce atoms were deposited from a thoroughly degassed tungsten filament onto a well prepared Ag(111) surface held inside a low-temperature STM in ultrahigh vacuum and cooled to 3.9 K by pumping on the He bath [18]. We used a cut PtIr wire as STM tip. Bias voltages U_s refer to the sample voltage with respect to the tip.

Figure 1(a) shows a large-scale STM topograph after deposition of about 1% of a monolayer of Ce onto Ag(111). Surprisingly, the Ce adatoms appear to form a hexagonal superlattice which is found everywhere on the sample, even at sample areas separated by a distance of 3 mm. We observe that this Ce superlattice covers the entire Ag(111) surface at a macroscopic scale. Figure 1(b) offers a closer

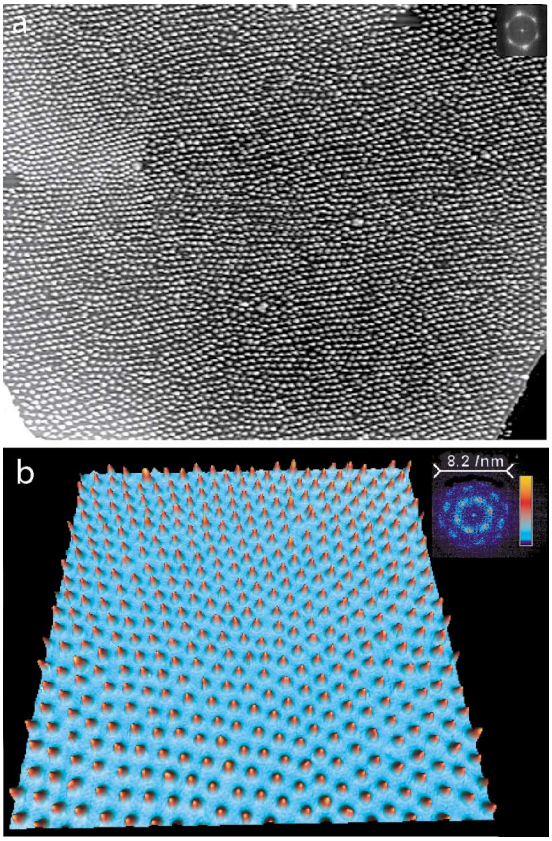

FIG. 1 (color). (a) Ce superlattice on Ag(111) at large scale at 4.8 K (240×192 nm^2; $U_s = -200$ mV, $I_s = 30$ pA). (b) The 3D STM image at 3.9 K (64×64 nm^2; $U_s = -100$ mV, $I_s = 10$ pA): Ce adatoms (red), Ag(111) (blue). Insets: the Fourier transforms of both images confirm the 2D hexagonal superlattice structure. (b) The horizontal line indicates the length in reciprocal space and the peak intensity is coded according to the color scale bar.

quasi-three-dimensional look on a typical region of the hexagonal Ce superlattice. The insets of Figs. 1(a) and 1(b) show the Fourier transform of both images confirming hexagonal order. The distance between two neighboring adatoms is determined from the real-space image to be 32 ± 0.5 Å. An increase of the sample temperature has a dramatic effect on the adatoms in their superlattice site. As shown in Fig. 2(a), at 3.9 K the Ce adatoms appear as stable protrusions, whereas already at 4.8 K they display a "frizzy" image indicating a finite adatom mobility. Immobile species at 4.8 K are also observed in Fig. 2(b), which are attributed to images of Ce dimers representing about ~5% of the number of adatoms [19]. Although the dimers appear to be close to the superlattice sites, they are rarely found precisely at the ideal locations. It is likely that the dimers appear to be close to superlattice sites because the surrounding mobile Ce atoms have adjusted their positions to best incorporate the fixed dimers into a superlattice. Figures 1 and 2 clearly show that surface defects (Ce dimers, dislocations, steps) locally perturb the long-range order of the adatom superlattice. Additional formation of Ce dimers was not observed at 4.8 K, pointing towards a repulsive interaction between Ce adatoms. Heating the sample up to 10 K causes the disappearance of the hexagonal superlattice. We note that deposition of Ce on Ag(100), which bears no surface state, does not lead to self-assembly of a superlattice.

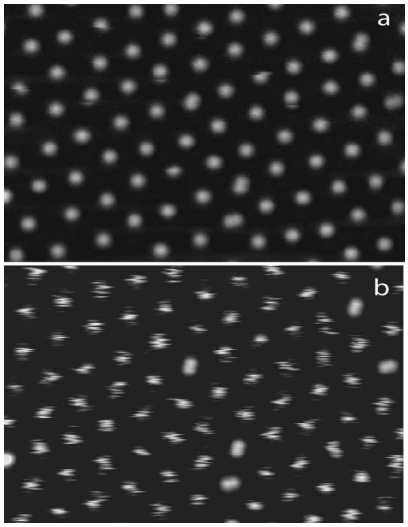

FIG. 2. High resolution STM images (32×21 nm^2; $U_s = -100$ mV, $I_s = 10$ pA) at 3.9 K (a) and 4.8 K (b). Ce adatoms form a hexagonal superlattice with an interadatom distance of 32 ± 0.5 Å. The superlattice is frozen at 3.9 K, whereas at 4.8 K adatoms are mobile around their superlattice site and only Ce dimers are stable.

In a first step of our analysis of the experimental results we evaluate the phase shift of the surface-state electrons at individual adatoms and dimers.

Figure 3(a) presents a STM image of an isolated Ce adatom at 3.9 K measured near the Fermi level at a tunnel bias of -3 mV. The circular electron density oscillations correspond to the well know standing-wave patterns near adsorbates on the (111) surfaces of noble metal surfaces [20]. The variation in the local density of states (Δ LDOS) at the Fermi level originating from the interference of incident and scattered surface-state electrons at adatom

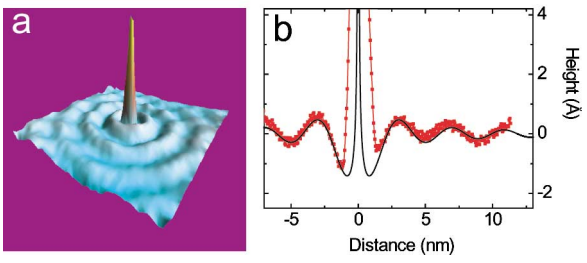

FIG. 3 (color online). (a) The 21×21 nm^2 3D STM image of a standing-wave pattern around an isolated Ce adatom on Ag(111) at 3.9 K ($U_s = -3$ mV, $I_s = 19$ pA). (b) Dotted line: topographic profile as a function of distance from a single Ce adatom. Solid line: fit using Eq. (1).

sites is given by [20]

$$\Delta\mathrm{LDOS}(\rho) \propto \frac{1}{k_F\rho}\left[\cos^2\left(k_F\rho - \frac{\pi}{4} + \delta_0\right) - \cos^2\left(k_F\rho - \frac{\pi}{4}\right)\right], \quad (1)$$

where $k_F = \sqrt{2m^*(-E_0)/\hbar^2}$ is the Fermi surface wave vector (0.0813 Å^{-1}) with the surface-state band edge $E_0 = -63$ meV for Ag(111) [21], ρ is the distance from the position of the center of an adatom, and $m^* = 0.40m_e$ [22] is the effective mass with m_e the free electron mass. The periodicity of the standing-wave oscillations at E_F is given by $\lambda_F/2 = 38$ Å. However, the distance of the first maximum of the LDOS from the adatom is determined by the scattering properties of the adatom. For a perfect scatterer, $\delta_0 = \pi/2$, the position of the first maximum of the LDOS oscillations at E_F would be at 38 Å. Our analysis, shown in Fig. 3(b), yields a value of $\delta_0 = (0.37 \pm 0.05)\pi$. Consequently, the scattering properties of the Ce adatoms determine the position of the first maximum in the electron density oscillations at E_F to be at a distance of 32 Å instead of 38 Å from the adatom.

Figure 4(a) presents a STM image of a hexagonally ordered domain of Ce adatoms and Ce dimers. Subsequently, the tip was used at increased tip-sample interaction ($U_s = 1.5$ V, $I_s = 20$ pA) to remove the Ce adatoms, but not dimers, from this area. The constant current image shown in Fig. 4(b) and taken near the Fermi level at a tunnel bias of -3 mV of the same region, reveals circular electron density oscillations near Ce dimers. The comparison between Figs. 4(b) and 4(c), which shows a modeling of the standing-wave pattern induced by the dimers with a phase shift $\delta_0 = (0.37 \pm 0.05)\pi$, indicates good agreement between experiment and model. Thus, the phase shifts for Ce adatoms and Ce dimers are practically identical.

Next, we model the observed hexagonal superlattice of Ce adatoms on Ag(111) by considering the interaction energy ΔE_{int} mediated by a Shockley surface-state band between two adatoms at a distance ρ on Ag(111) [14]:

$$\Delta E_{\mathrm{int}}(\rho) \simeq -AE_0\left(\frac{2\sin(\delta_0)}{\pi}\right)^2 \frac{\sin(2k_F\rho + 2\delta_0)}{(k_F\rho)^2}, \quad (2)$$

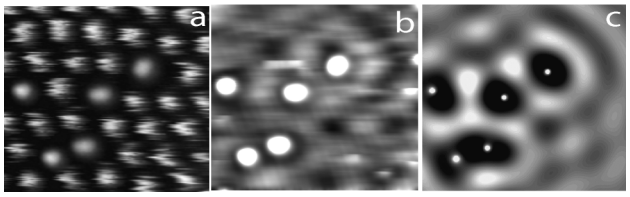

FIG. 4. (a),(b) Successive constant current STM images (20 nm × 17 nm) of Ce on Ag(111). (a) Hexagonal superlattice ($U_s = -100$ mV, $I_s = 30$ pA). (b) Standing wave pattern near Ce dimers ($U_s = -3$ mV, $I_s = 20$ pA). (c) Calculated local electron density (see text).

where A is a scattering amplitude as defined in Ref. [12] that expresses scattering from surface into bulk states. For ΔE_{int} to have its deepest minimum at the measured Ce adatom distance of 32 Å, we need $\delta_0 = 0.37\pi$, in excellent agreement with the analysis of the standing-wave oscillations at the Fermi energy.

In the third step of our analysis we determine directly the superlattice confining potential by making a detailed statistical analysis of the mobile Ce atoms as they hop around the nominal threefold coordinated lattice sites. Figure 5(b) presents a 2D map of the calculated potential E_{pot} obtained by superposition of six external adatom two-body interaction energies of the hexagonal superlattice at the location of the central adatom. Since at 4.8 K the Ce adatoms randomly hop from one atomic position to another within the well, we can estimate A (and hence the well depth) by measuring the statistical distribution of adatom positions x and fitting to a Boltzmann distribution, $e^{-E_{\mathrm{pot}}(x)/k_BT}$. To this end, we analyzed about 3700 adatom topographic cross sections (about 16 per adatom) and made a histogram of an adatom's displacement relative to its average position, as shown in Fig. 5(a). This measured distribution should approximate the true adatom distribution provided $\tau_{\mathrm{tip}} \ll \tau_{\mathrm{hop}} \ll \tau_{\mathrm{atom}}$, where $\tau_{\mathrm{tip}} = 30$ ms is the time to scan over a single adatom, τ_{hop} is the characteristic adatom hopping time from one Ag(111) threefold site to another, and $\tau_{\mathrm{atom}} = 16$ s is the total time during which a given adatom is monitored. We estimated $\tau_{\mathrm{hop}} = 300 \pm 100$ ms at 4.8 K from the statistical probability of observing a hop during τ_{tip}, and the

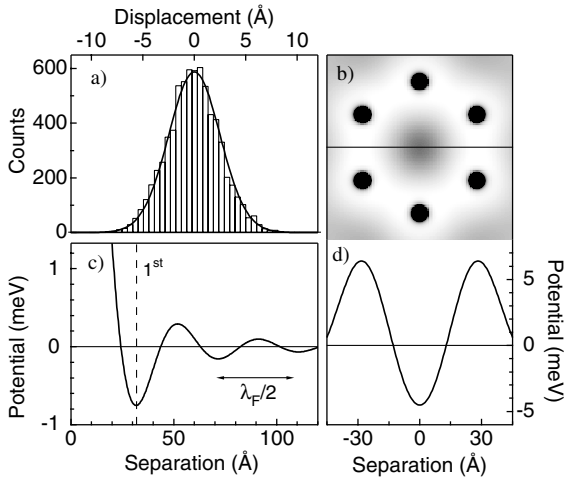

FIG. 5. (a) Histogram of measured Ce adatom displacements at 4.8 K with respect to the hexagonal superlattice sites and statistical analysis (full curve). (b) The 2D representation of the deduced potential induced by the six external atoms of the hexagonal superlattice at the location of the central Ce adatom. The filled circles arise from the divergence of the two-body potential at the adatom position. (c) Two-body interaction energy of Ce adatoms on Ag(111). The position of the first neighbor adatoms at 32 Å is marked. (d) Cross section of the potential (b) along the horizontal line (see text).

probability of observing no jumps during the 1 s between successive scans over a given adatom. The measured Gaussian distribution is consistent with the approximately parabolic potential well [see Fig. 5(d)], and the measured full width at half maximum of 5.8 ± 0.2 Å indicates a value of $A = 0.27 \pm 0.03$. Our analysis of the interaction energy including two- and three-body interactions [14,15] yields essentially the same result. This allows us to quantify the energy scale in Fig. 5(d), from which we find a potential well depth of 4.9 ± 0.5 meV and a trapping barrier height of 11.8 ± 1.2 meV. Our values of $A = 0.27$ and $\delta_0 = 0.37\pi$ are in good agreement with values obtained by Knorr *et al.* [12] for Co on Ag(111) by analyzing the pair correlation function at very low Co coverage. Our experiments show that an adatom phase shift of $\delta_0 = 0.37\pi$, which is close to the value $\delta_0 = \pi/3$ for Co/Ag(111), permits the formation of the Ce superlattice on Ag(111). We note that the time $\tau_{\text{hop}} = 300$ ms at 4.8 K suggests an adatom diffusion barrier of 11 meV, assuming a 10^{12} s^{-1} diffusion prefactor. In this situation, it is possible to find a temperature ($\sim$4.8 K in our case) at which the adatoms can hop between adjacent Ag(111) sites many times at a reasonably fast rate without leaving the potential well, thus favoring superlattice formation. These barrier heights correspond well to the measured hopping rate at 4.8 K, and to the experimentally observed disappearance of the superlattice at $T \sim 10$ K.

The deduced two-body interaction energy $\Delta E_{\text{int}}(\rho)$ is presented in Fig. 5(c). At small adatom separation a strong repulsion between the adatoms prevents dimer formation. The first minimum at 32 Å and -0.8 meV depth corresponds to the position of the first neighbor adatom of the hexagonal superlattice, which is formed because the thermal energy at 4.8 K is sufficient to overcome the repulsive barrier ($\sim$0.3 meV) at 55 Å. Our analysis shows that the hexagonal superlattice is most stable at 4.8 K if practically all available superlattice sites are occupied by Ce adatoms. Consequently, and in agreement with our experimental observations, at low Ce adatom concentration ($\ll 10^{-2}$ ML) the hexagonal superlattice does not self-organize. Thus, sample temperature, low adatom diffusion barrier and adatom concentration are the key parameters for successful self-assembly of the atomic superlattice. In a kind of autocatalytic process, the Ce adatoms need sufficient thermal energy to overcome the outer potential barriers and, simultaneously, high enough concentration to form the necessary potential well depth to lock in the first minimum at nearest neighbor distance.

We have created a two-dimensional self-assembled hexagonal superlattice of metallic Ce adatoms. In fact, this superlattice may represent a 2D Kondo lattice where the electrons in the 2D surface-state band of Ag(111) are also involved in the indirect exchange coupling between the spins of the magnetic adatoms. Variation of support and of magnetic adatoms may allow us to tune the lattice constant of the superlattice thereby forming ferromagnetic or antiferromagnetic adatom pairs at different separations. Evidently, the success of such an approach will crucially depend on the relative strength of the electronic versus the magnetic interactions. A recent calculation for Co/Ag(111) [23] predicts oscillatory magnetic interactions to be about 2 orders of magnitude smaller than the electron density mediated ones. An observation of the spin-spin interactions would therefore require temperatures in the milli-Kelvin range. However, such a 2D Kondo lattice may be of interest for electron-spin based quantum computing. The ability to control the long-range order of magnetic adatoms opens new possibilities for the investigation of two-dimensional magnetism and for the development of atomic-scale magnetic devices.

This work has been supported by the Swiss National Science Foundation.

*Present address: University of Oxford, Department of Materials, Parks Road, Oxford OX1 3PH, U.K.

[1] D. M. Eigler and E. K. Schweizer, Nature (London) **344**, 524 (1990).
[2] H. C. Manoharan, C. P. Lutz, and D. M. Eigler, Nature (London) **403**, 512 (2000).
[3] A. J. Heinrich, C. P. Lutz, J. A. Gupta, and D. M. Eigler, Science **298**, 1381 (2002).
[4] N. Nilius, T. M. Wallis, and W. Ho, Science **297**, 1853 (2002).
[5] G. M. Whitesides and B. Grzybowski, Science **295**, 2418 (2002).
[6] H. Zeng *et al.*, Nature (London) **420**, 395 (2002).
[7] C. T. Black, C. B. Murray, R. L. Sandstrom, and Shouheng Sun, Science **290**, 1131 (2000).
[8] K. H. Lau and W. Kohn, Surf. Sci. **75**, 69 (1978).
[9] T. T. Tsong, Phys. Rev. Lett. **31**, 1207 (1973).
[10] E. Wahlström, I. Ekvall, H. Olin, and L. Walldén, Appl. Phys. A **66**, S1107 (1998).
[11] J. Repp *et al.*, Phys. Rev. Lett. **85**, 2981 (2000).
[12] N. Knorr *et al.*, Phys. Rev. B **65**, 115420 (2002).
[13] A. Zangwill, *Physics at Surfaces* (Cambridge University Press, Cambridge, U.K., 1988), pp. 279–280.
[14] P. Hyldgaard and M. Persson, J. Phys. Condens. Matter **12**, 13 (2000).
[15] P. Hyldgaard and M. Persson, Europhys. Lett. **59**, 265 (2002).
[16] J. Repp, Ph.D. thesis, Free University of Berlin, 2002.
[17] M. M. Kamna, S. J. Stranick, and P. S. Weiss, Science **274**, 118 (1996).
[18] R. Gaisch *et al.*, Ultramicroscopy **42**, 1621 (1992).
[19] The present investigation suggests that the measurements of J. Li *et al.*, Phys. Rev. Lett. **80**, 2893 (1998), were probably performed on Ce dimers.
[20] M. F. Crommie, C. P. Lutz, and D. M. Eigler, Nature (London) **363**, 524 (1993).
[21] M. Pivetta *et al.*, Phys. Rev. B **67**, 193402 (2003).
[22] J. Li, W.-D. Schneider, and R. Berndt, Phys. Rev. B **56**, 7656 (1997).
[23] L. Niebegrall *et al.*, Verh. Dtsch. Phys. Ges. **38**, 5/411 (2003).